Biaxial mechanical properties of bovine jugular venous valve leaflet tissues

Hsiao-Ying Shadow Huang & Jiaqi Lu

Biomechanics and Modeling in Mechanobiology

ISSN 1617-7959

Biomech Model Mechanobiol
DOI 10.1007/s10237-017-0927-1

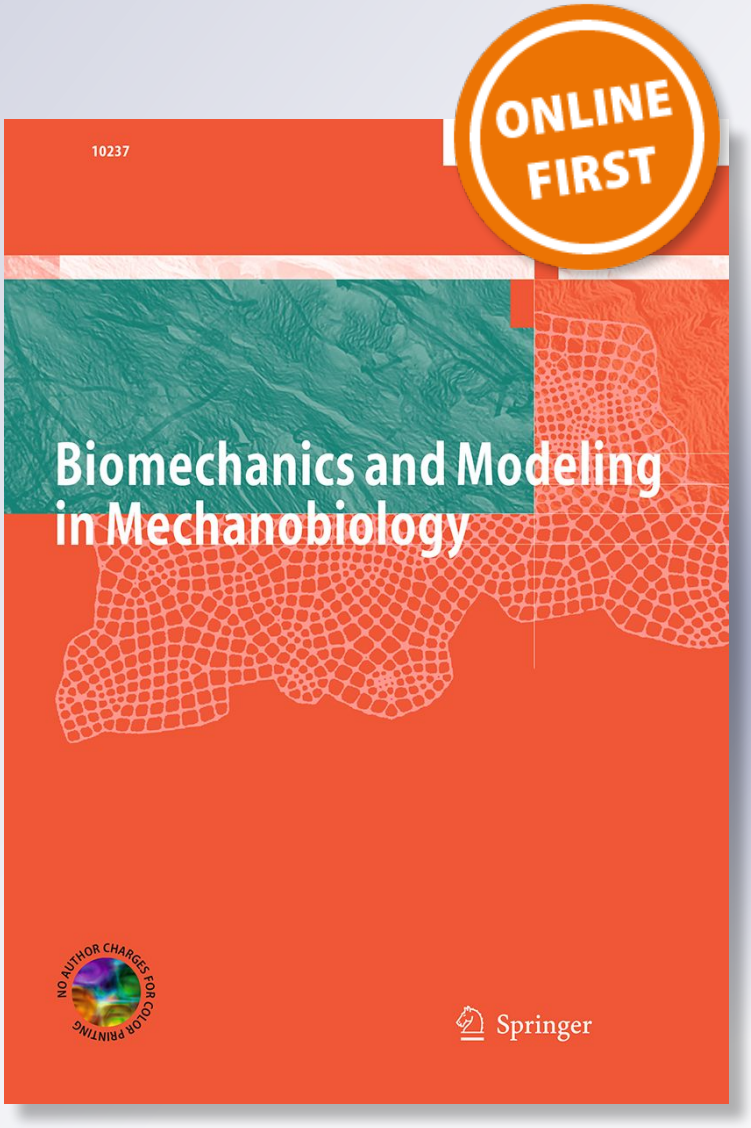

Springer

Biomech Model Mechanobiol
DOI 10.1007/s10237-017-0927-1

ORIGINAL PAPER

Biaxial mechanical properties of bovine jugular venous valve leaflet tissues

Hsiao-Ying Shadow Huang[1] · **Jiaqi Lu**[1]

Received: 25 October 2016 / Accepted: 9 June 2017

Abstract Venous valve incompetence has been implicated in diseases ranging from chronic venous insufficiency (CVI) to intracranial venous hypertension. However, while the mechanical properties of venous valve leaflet tissues are central to CVI biomechanics and mechanobiology, neither stress–strain curves nor tangent moduli have been reported. Here, equibiaxial tensile mechanical tests were conducted to assess the tangent modulus, strength and anisotropy of venous valve leaflet tissues from bovine jugular veins. Valvular tissues were stretched to 60% strain in both the circumferential and radial directions, and leaflet tissue stress–strain curves were generated for proximal and distal valves (i.e., valves closest and furthest from the right heart, respectively). Toward linking mechanical properties to leaflet microstructure and composition, Masson's trichrome and Verhoeff–Van Gieson staining and collagen assays were conducted. Results showed: (1) Proximal bovine jugular vein venous valves tended to be bicuspid (i.e., have two leaflets), while distal valves tended to be tricuspid; (2) leaflet tissues from proximal valves exhibited approximately threefold higher peak tangent moduli in the circumferential direction than in the orthogonal radial direction (i.e., proximal valve leaflet tissues were anisotropic; $p < 0.01$); (3) individual leaflets excised from the same valve apparatus appeared to exhibit different mechanical properties (i.e., intra-valve variability); and (4) leaflets from distal valves exhibited a trend of higher soluble collagen concentrations than proximal ones (i.e., inter-valve variability). To the best of the authors' knowledge, this is the first study reporting biaxial mechanical properties of venous valve leaflet tissues. These results provide a baseline for studying venous valve incompetence at the tissue level and a quantitative basis for prosthetic venous valve design.

Keywords Anisotropy · Tissue biomechanics · Biaxial testing · Chronic venous insufficiency

1 Introduction

Venous valves are designed to ensure one-way blood flow like their cardiac counterparts; similarly, they permit non-physiologic reflux when rendered incompetent or absent by disease (Gottlob and May 1986). In the saphenous, popliteal and femoral veins and their tributaries, venous valve incompetence lets gravity exert its full force on the column of blood between the right heart and the calves, commonly progressing from varicose veins to debilitating chronic venous insufficiency (CVI) (Bergan 2008; Edwards and Edwards 1940; Zervides and Giannoukas 2012). In the jugular veins, venous valve incompetence has been associated with idiopathic diseases ranging from intracranial hypertension (Nedelmann et al. 2009) to transient global amnesia (Lochner et al. 2014). Yet while CVI alone afflicts a significant percentage of adults (Zervides and Giannoukas 2012) and increases with pregnancy (James et al. 1996; Sparey et al. 1999) and age (Beebe-Dimmer et al. 2005; Fan 2005), the rational design and clinical assessment of functional prosthetic (de Borst and Moll 2012; de Borst et al. 2003; DeLaria et al. 1993; Hill et al. 1985; Moriyama et al. 2011; Reeves et al. 1997) and tissue-engineered (Brountzos 2003; Glynn et al. 2016; Jones et al. 2012; Kehl et al. 2016; Kuna et al. 2015; Pavcnik 2002; Shen 2014; Teebken et al. 2003, 2009; Weber 2014; Wen 2012; Yuan 2013) venous

✉ Hsiao-Ying Shadow Huang
hshuang@ncsu.edu

[1] Department of Mechanical and Aerospace Engineering, North Carolina State University, R3158 Engineering Building 3, Campus Box 7910, 911 Oval Drive, Raleigh, NC 27695, USA

Published online: 19 June 2017

valves lag behind that of the ubiquitous replacement heart valve.

Kistner (1968) pioneered the surgical reconstruction of venous valves, and Hill et al. (1985) demonstrated the feasibility of synthetic and prosthetic venous valves. Toward a practical bioprosthesis, DeLaria et al. (1993) evaluated venous valves from ovine, equine, and bovine jugular veins, and electrospun polymer venous valves capable of percutaneous delivery have been demonstrated in vitro (Moriyama et al. 2011). In arguably the first tissue engineering-based approach, Pavcnik and colleagues have been evaluating the in vivo remodeling of stent-mounted, small intestinal submucosa-based venous valves since 2000 (Brountzos 2003; Glynn et al. 2016; Jones et al. 2012; Pavcnik et al. 2000; Pavcnik 2002). Meanwhile, Teebken et al. (2003, 2009) were the first to use a bioreactor to repopulate decellularized jugular valves prior to implantation. More recently, Weber (2014) engineered venous valves using poly(glycolic acid) scaffolds, and Zhang and colleagues repopulated decellularized valves with bone marrow cells (Shen 2014; Wen 2012; Yuan 2013). However, while promising, current venous valve replacements have been designed without the benefit of venous valve leaflet tissue mechanical properties, which remain largely unknown.

To the best of the authors' knowledge, only a single study by Ackroyd et al. (1985) has reported mechanical properties of venous valve *leaflet tissue* and only insofar as uniaxial tensile strength and failure strain. Reeves et al. (1997) and Rittgers et al. (2007) reported on the *in situ* fluid mechanics of native, lyophilized, and polymer venous valves, and Kuna et al. (2015) recently reported suture tearing forces for human femoral vein valves. However, no stress–strain curves or tangent moduli have been published for venous valve leaflet tissues, let alone the biaxial assessments that would be required to retain the effects of axial coupling. Characterizing the biaxial mechanical behavior of venous valve leaflet tissue is critical to understanding the opening and closing mechanisms in healthy and diseased venous valves (Buescher et al. 2005; Karino and Motomiya 1984; Lurie et al. 2003; Qui et al. 1995) and the hypertension-mediated pathogenesis of venous valve distension and incompetence (Bernardini et al. 2010; Edwards and Edwards 1940; Qureshi 2015). Further, biaxial mechanical properties will aid in designing not only native-like venous valve replacements, but venous-derived bioprosthetic heart valves as well (Noishiki 1993). Indeed, Medtronic's Contegra® pulmonary valved conduit (Carrel 2004; Corno et al. 2001) and transcatheter Melody® pulmonary valve (McElhinney and Hennesen 2013) are based on glutaraldehyde-fixed trileaflet bovine jugular venous valves.

Toward refining tissue-level principles of venous valve function and valve replacement, in the current study, biaxial mechanical test methods we developed for heart valve leaflets (Huang et al. 2012, 2014; Huang and Huang 2015) were adapted to venous valve leaflets excised from bovine jugular veins. Equibiaxial tests were conducted at a strain magnitude of 60% in both circumferential and radial directions, and leaflet tissue stress–strain curves were generated for proximal and distal venous valves (i.e., valves closest and furthest from the right heart, respectively). Moreover, toward linking venous valve leaflet tissue mechanical properties to underlying microstructure and composition, histological evaluation of Masson's trichrome and Verhoeff–Van Gieson stained tissues was performed, and soluble collagen concentrations were measured biochemically (Huang et al. 2012).

2 Materials and methods

2.1 Preparation of venous valve leaflet tissues from bovine jugular veins

Bovine jugular veins were obtained from an abattoir. Justifications for testing venous valves from jugular veins include their relatively large size (~1.5 cm dia. vein (DeLaria et al. 1993; Qui et al. 1995); leaflets ~150 mm^2), their association with intracranial hypertension (Nedelmann et al. 2009) to transient global amnesia (Lochner et al. 2014), and their clinical relevance in prosthetic venous valves (DeLaria et al. 1993; Qui et al. 1995). Tissues from cows (Holstein breed, female, 10+ years old, ~1250 lbs weight) used in meat production were shipped overnight on ice, ~24 h post-slaughter. Jugular vein samples were ~30 cm in length, with diameters ranging from 1.5 to 1.7 cm (Fig. 1a). After trimming off loose connective tissue, two pairs of tweezers were used to evert (i.e., turn inside-out) the veins to expose the venous valves, thereby facilitating leaflet dissection. The proximal end of the vein (i.e., that closest the right heart) was identified by the semilunar shape of the leaflets (Fig. 1a), and venous valves were grouped according to their location along the length of the vein, such that potential proximal-to-distal differences in their properties could be assessed (i.e., inter-valve variability). Measuring from the center of the proximal-most venous valve's basal attachment, the first 10-cm portion of each jugular vein sample was defined as "proximal," the second 10-cm portion "middle," and the last portion "distal" (Fig. 1a). With the vein spread flat on a cutting board, individual leaflets were lifted by their free edge with a pair of tweezers and excised by cutting along their semilunar basal attachment (Fig. 1b). Following an established method from previous studies (Billiar and Sacks 2000; May-Newman et al. 2009; Van Geemen et al. 2012), leaflet thicknesses were measured in the central belly region using a 1010Z dial indicator pocket gauge (Starrett Co., Athol, MA). During the dissection process, both bicuspid and tricuspid valves were observed in jugular vein samples, and intra-valve variability was assessed

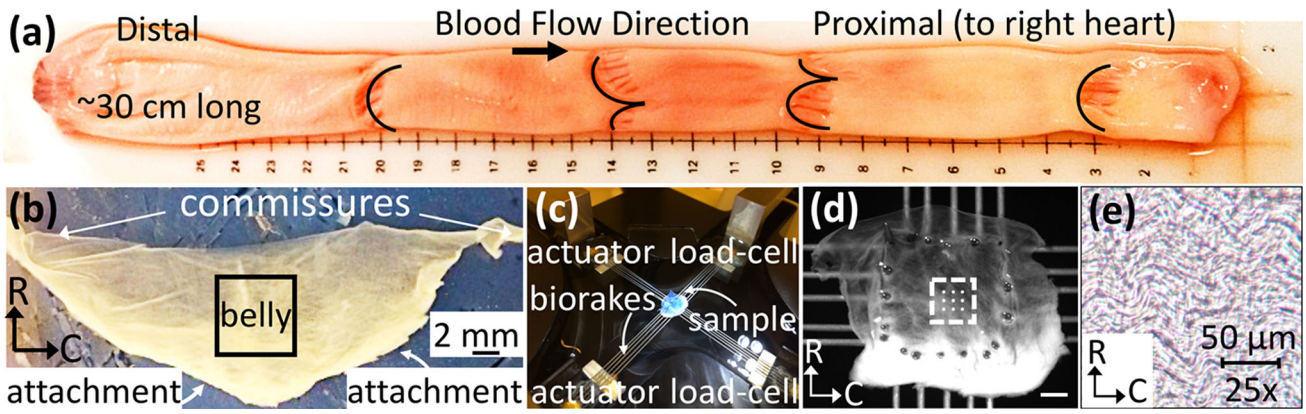

Fig. 1 **a** Bovine jugular vein and associated venous valve leaflets (basal attachments traced in black to facilitate identification). Of note, intact leaflets are only partly visible because the veins were everted during leaflet excision. **b** Excised venous valve leaflet. *C* Circumferential, *R* radial direction. **c** The BioTester is equipped with load cells and actuators for each axis. **d** Data points inside the *dashed square* are output for stress/strain quantification. *Scalebar* = 1 mm. **e** Crimped collagen fibers were observed to be aligned principally along the circumferential direction, as observed by phase-contrast microscopy of whole-mount, unstained leaflets. *Scalebar* = 50 µm

(i.e., differences between the two (bicuspid) or three (tricuspid) individual leaflets excised from the same venous valve apparatus).

2.2 Biaxial mechanical testing of venous valve leaflet tissues

To minimize potential boundary effects, only the central belly region of each leaflet was tested. Tissue from the central belly region of each leaflet was trimmed into a 7 mm × 7 mm square, oriented such that the orthogonal axes of each square specimen corresponded with the circumferential (C) and radial directions (R) of the venous valve. A biaxial tester, the BioTester 5000 (CellScale, Waterloo, Ontario, Canada), equipped with two load cells (one per axis of loading; 10±0.02 N) was used for biaxial mechanical testing (Fig. 1c) (Huang et al. 2012, 2014; Huang and Huang 2015). Synchronized time lapse video for real-time monitoring and post-process analysis was provided by a charge-coupled device (CCD) camera, which acquired images with a pixel resolution of 1280 × 960, an acquisition rate of 15 Hz, and a lens focal length of 75 mm. Data logging capabilities ensured registration of axis loads, displacements, and image frames. Image tracking and analysis software (LabJoy, CellScale) was then used to review images collected during biaxial testing. Each of the four edges of the 7 mm × 7 mm square tissue sample was gripped by a CellScale BioRake, piercing each tissue edge with five rigid tungsten "tines" and restricting sample shear deformation (Fig. 1c, d). Gripped samples were lowered into a temperature-controlled (37 °C) bath of Hank's balanced salt solution (HBSS). Pre-loading and pre-conditioning were anticipated to release sample internal residual stresses (Davis and De Vita 2012). Samples were therefore pre-loaded to 0.01 N and then pre-conditioned at 1%/s to 30% strain for ten cycles to generate repeatable and reliable results, followed by a 5-min recovery period. Tissue samples were then stretched at a rate of 1%/s to an equibiaxial strain of 60% and recovered back to 0% strain, during which displacement and force data were collected. The biaxial strain magnitude of 60% was chosen based on our preliminary testing, in which we found 60% strain did not result in tissue failure. To minimize potential boundary effects, markers inside the central 3 mm × 3 mm region of the tissue sample were used to calculate displacements (dashed box in Fig. 1d). Based on the sample dimensions and output data, corresponding nominal stress (i.e., first Piola–Kirchhoff stress) and true strain values were calculated and stress–strain curves were plotted. The peak tangent modulus was calculated in the relatively linear region of the stress–strain curve between 45 and 60% strain by subtracting the stress at 45% strain from the stress at 60% strain and then dividing the difference by the corresponding difference in strain magnitude (i.e., 15%). The peak stress was defined as the stress magnitude recorded at 60% strain.

2.3 Histological assessment of venous valve leaflet tissues

Prior to preparing samples for histological assessment, whole-mount, unstained tissues were imaged under phase contrast (VistaVision, VWR, West Chester, PA, USA), and crimped collagen fibers were observed to be aligned principally along the circumferential direction of the samples (Fig. 1e). Histological photomicrographs of jugular venous valve leaflet samples were prepared as follows: Jugular venous valve tissues from the proximal and distal groups were fixed in 10% (v/v) buffered formalin and submitted to

the Histology Laboratory in the NC State College of Veterinary Medicine. Venous valve leaflet tissues were paraffin embedded, sectioned, and stained by either hematoxylin and eosin (H&E), Masson's trichrome, or Verhoeff–Van Gieson (VVG) protocols. In H&E stained sections, extracellular matrix (including collagens) is pink and nuclei are blue to black. In Masson's trichrome stained sections, collagen is blue, nuclei are black, and cytoplasm is red. In VVG stained sections, elastic fibers are black, collagen is red, cytoplasm is yellow, and nuclei are black. Slides were imaged on a Zeiss Axiophot optical microscope (Carl Zeiss AG, Oberkochen, Germany) at 400x original magnification (Huang et al. 2012, 2007).

2.4 Biochemical analysis of venous valve leaflet tissue collagen concentration

Twenty-two specimens from the proximal group, 16 from the middle group, and 22 from the distal group were collected for biochemical analysis of collagen concentration. Collagen concentrations (an aggregate of collagen types I, III, and V) in the jugular venous valve leaflets were determined via an assay kit (Sircol; Accurate Chemical and Scientific Corp., Westbury, NY, USA) using techniques adapted from our previous study (Huang et al. 2012) and other papers (Engelmayr et al. 2005). In brief, the specimens ($\sim 1 \times 1$ mm^2) from each venous valve leaflet tissue were frozen after mechanical testing. The samples were weighed using an analytical balance (VWR, West Chester, PA, USA). Specimens were extracted in an acetic acid (0.5 M; Sigma-Aldrich, St. Louis, MO, USA) and pepsin (1 mg/ml Pepsin A [P-7000]; Sigma-Aldrich, St. Louis, MO, USA) solution (Huang et al. 2012). A pilot study was performed to determine the amount of time required to extract the maximum amount of soluble collagen from venous valve leaflet tissues. Pilot study results showed that the apparent collagen concentration plateaued by 120 h of extraction, with no significant differences observed at 144 h. Collagen extraction solution (1 ml) was added to each tube, and samples were placed on a vortex mixer (VWR, West Chester, PA, USA) for 120 and 144 h, respectively. The collagen concentration was quantified based on the pre-calculated collagen standard curve described in our previous work (Huang et al. 2012). Briefly, a collagen standard curve ($y = 0.0284x$, $R^2 = 0.9994$) was established using four absorbance values from the standards, where y is the absorbance value at 550 nm, x is the mass of collagen, and R is the correlation coefficient between x and y. The collagen masses of the 60 experimental samples were calculated by comparing absorbance values to those of the collagen standards measured via a spectrophotometer (Thermo Fisher Scientific, Waltham, MA, USA). The collagen concentration of each sample was then calculated by normalizing to the wet weight of the sample.

2.5 Statistics

Statistical analyses were conducted using JMP software (SAS Institute Inc. Cary, NC, USA). Comparisons involving one factor (e.g., venous valve location on the distal-to-proximal axis or individual leaflets excised from the same venous valve apparatus) were conducted using one-way ANOVA, with Tukey's post hoc test for significance ($p < 0.05$) of multiple comparisons. To test for venous valve leaflet tissue anisotropy, paired t tests were used to compare peak tangent moduli and peak stresses in the circumferential and radial directions. Data are presented as mean ± standard deviation.

3 Results

3.1 Preparation of venous valve leaflet tissue results

Venous valve leaflets were excised from bovine jugular veins following eversion (i.e., turning inside-out), so as to facilitate identification of the leaflet margins and thereby mitigate damage during excision. During the dissection process, different vein samples contained different numbers of valves. In each of the vein samples, at least one valve was observed near the proximal end. However, valves in the middle and distal portions of the vein were not as frequently observed. Both bicuspid and tricuspid valves were observed during the dissection process, with proximal valves generally bicuspid and distal valves generally tricuspid. Specifically, in 66% of the collected veins, at least one tricuspid valve was observed, and 37.5% of the veins containing a tricuspid valve had more than one tricuspid valve. On average, venous valve leaflets excised from the bovine jugular vein were ~25−39 mm long in the circumferential direction, 8–10 mm long in the radial direction, and ~50 μm thick at the belly region (Fig. 1b).

3.2 Biaxial mechanical testing results

Mean stress–strain responses for proximal ($n = 11$), middle ($n = 8$) and distal ($n = 11$) venous valve leaflet tissues showed clear evidence of nonlinearity and circumferential–radial anisotropy (Fig. 2). As is typical for many soft collagenous tissues, three distinct stress–strain response regions were evident: a relatively linear, low tangent modulus toe region between 0 and ~25% strain, an exponential transition region between ~25 and ~45% strain, and a higher tangent modulus, relatively linear region between ~45 and 60% strain (i.e., the peak applied strain). Peak tangent moduli and peak stresses at 60% strain are listed in Table 1, and comparisons between parameters are illustrated in Fig. 3a and b, respectively.

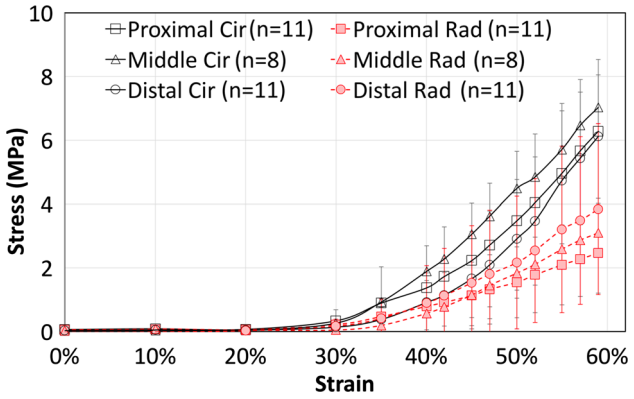

Fig. 2 Equibiaxial stress–strain curves for venous valve leaflet tissues from the bovine jugular vein. The tensile mechanical responses of tissues derived from proximal, middle and distal valves were each nonlinear in both the circumferential and radial directions, exhibiting a relatively linear, low tangent modulus toe region between 0 and ~25% strain, an exponential transition region between ~25 and ~45% strain, and a higher tangent modulus, relatively linear region between ~45 and 60% strain (i.e., the peak applied strain). Further, venous valve tissues exhibited pronounced anisotropy, as evidenced by the distinctly higher slopes of the circumferential stress–strain curves (*black*) relative to those of the radial direction (*red*)

For the proximal venous valve leaflet tissue samples, the circumferential direction exhibited a peak tangent modulus of 27 ± 9 MPa, which on average was ~threefold higher than that of the radial direction, 9 ± 6 MPa ($p = 0.0001$). For middle tissue samples, the circumferential direction exhibited a peak tangent modulus of 24 ± 20 MPa, which on average trended ~twofold higher than that of the radial direction, 10 ± 16 MPa. Similarly, for distal tissue samples, the circumferential direction exhibited a peak tangent modulus of 30 ± 6 MPa, which trended ~twofold higher than that of the radial direction, 15 ± 9 MPa. Of note, while the ratio of circumferential-to-radial peak tangent modulus appeared to be higher in the proximal samples (i.e., ~3:1) when compared with that of the middle and distal samples (i.e., ~2:1), differences did not reach statistical significance (Fig. 3a). Similarly, while there appeared to be a slight trend of increased radial peak tangent modulus on going from proximal to distal, differences did not reach statistical significance (Fig. 3a; Table 1). Similar to the peak tangent modulus results, the proximal group exhibited significantly larger peak stress at 60% strain in the circumferential direction than in the radial ($p = 0.0003$), with trends of higher circumferential stress in the middle and distal groups (Fig. 3b; Table 1). However, no significant differences in either the circumferential or radial peak stresses at 60% strain were observed between the proximal, middle and distal groups. Overall, inter-valve variability in biaxial mechanical properties was not detected in the context of the samples tested herein.

Recognizing that individual biaxial test results naturally differ to some degree due to experimental variability, in evaluating individual sample stress–strain curves, the two (bicuspid) or three (tricuspid) leaflets from the same valve apparatus appeared to exhibit differences in mechanical properties. In an initial attempt to assess for potential intra-valve variability, we compared the mechanical properties of leaflet tissues excised from the same valve apparatus by dividing samples into two groups: (1) low: those with the lowest measured peak tangent modulus (or peak stress at 60% strain) and (2) high: those with the highest peak tangent modulus (or peak stress at 60% strain). By this method of sample grouping, trends were found between the low and high groups, including: a trend of higher radial peak tangent modulus in the high group versus the low group for distal leaflets (Fig. 3c), a trend of higher circumferential peak stress at 60% strain in the high group versus the low group for proximal leaflets, and a trend of higher radial peak stress at 60% strain in the high group versus the low group for distal leaflets (Fig. 3d). No significant differences in either the peak tangent modulus or peak stress at 60% strain were observed in the middle group (Fig. 3c, d).

3.3 Histological results

Consistent with the observed nonlinear, anisotropic stress–strain responses, photomicrographs of venous valve leaflet tissues showed evidence of collagen fiber crimp (i.e., undulations) and collagen fiber alignment (Fig. 4). Qualitatively, collagen fiber alignment appeared to be more pronounced in proximal (Fig. 4a–c) than distal samples (Fig. 4d–f); however, future studies will be needed to quantify said observations across multiple photomicrographs for statistical comparison.

3.4 Collagen assay results

Pilot studies (not shown) indicated that acid–pepsin solubilization of collagen plateaued by 120 h. No significant

Table 1 Peak tangent moduli (in the 45–60% strain range) and peak stresses (at 60% strain) measured for venous valve leaflet tissues excised from bovine jugular veins

	Proximal ($n = 11$)		Middle ($n = 8$)		Distal ($n = 11$)	
	Cir	Rad	Cir	Rad	Cir	Rad
Peak tangent modulus (MPa)	27 ± 9	9 ± 6	24 ± 20	10 ± 16	30 ± 6	15 ± 9
Peak stress at 60% strain (MPa)	6 ± 2	2.5 ± 1	6 ± 6	2.4 ± 4	6 ± 2	4 ± 3

Mean ± standard deviation

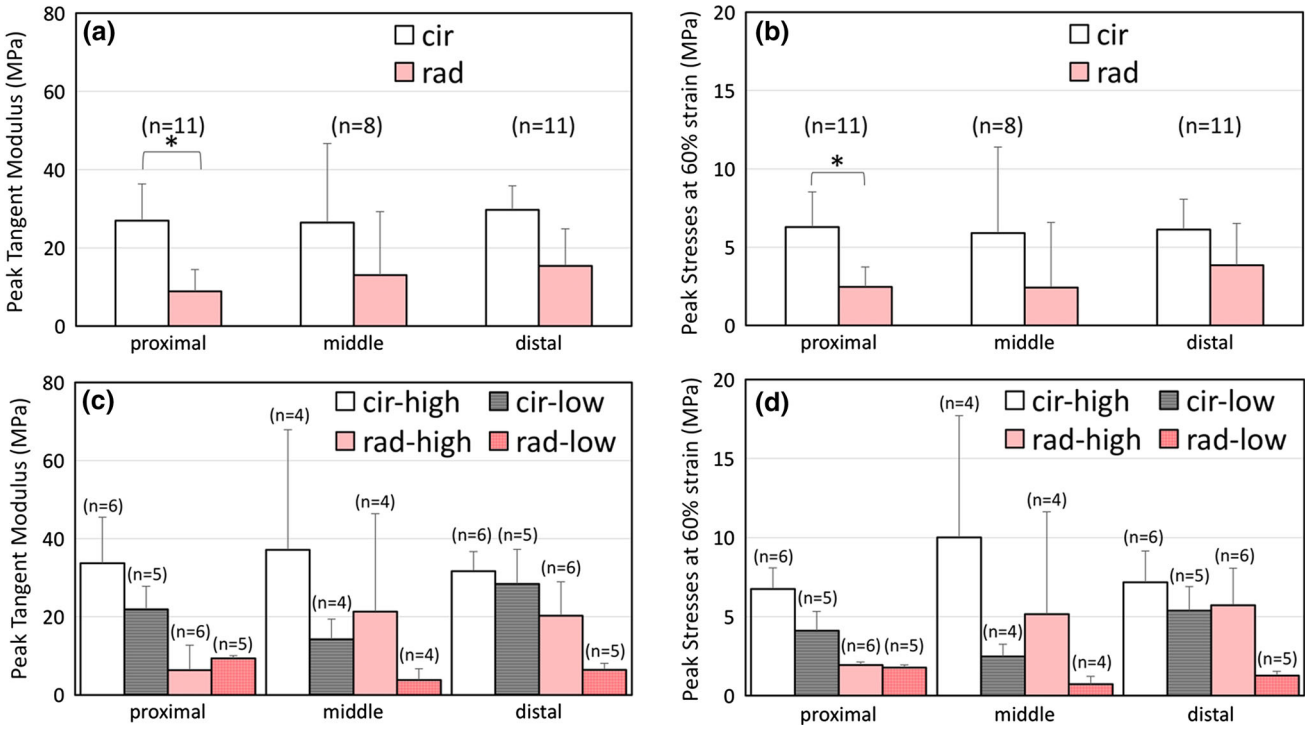

Fig. 3 Inter-valvular and intra-valvular variability in peak tangent moduli (in the 45–60% strain range) and peak stress values (at 60% strain) for jugular venous valve tissues. **a**, **b** Significant differences in peak tangent modulus and peak stress values at 60% strain between the circumferential and radial directions were found in the proximal group ($p < 0.01$), with trends of anisotropy in the middle and distal groups. However, no significant inter-valvular variability between the three groups was observed. **c** A trend of higher radial peak tangent modulus was observed in the high group versus the low group for distal samples, suggesting intra-valvular variability may exist. **d** A trend of higher circumferential peak stress was observed in the high group versus the low group in proximal samples, and a trend of higher radial peak stress was observed in the high group versus the low group for distal samples, suggesting intra-valvular variability may exist

differences in apparent collagen concentration were observed between the 120- and 144-h extraction time groups, indicating that 120 h was sufficient to extract all of the acid–pepsin soluble collagen from bovine jugular vein venous valve leaflets (Fig. 5). Trends were found between the proximal and distal groups at 120 h, with distal valves (495,000 ± 199,000 μg/g wet weight) appearing to have a higher mean collagen concentration than proximal valves (307,000 ± 165,000 μg/g wet weight). Leaflet tissues from middle valves had an intermediate collagen concentration (339,000 ± 122,000 μg/g wet weight). Moreover, trends were observed among all three groups at 144 h. Distal valves (544,000 ± 234,000 μg/g wet weight) appeared to have a higher mean collagen concentration than middle valves (381,000 ± 106,000 μg/g wet weight), which in turn appeared to have a higher collagen concentration than proximal valves (301,000 ± 172,000 μg/g wet weight). In a separate set of collagen assays on 16 lyophilized venous valve leaflets (i.e., dry weight-based measurements), we observed a similar trend of increased mean collagen concentration in proximal valves versus middle and distal valves: proximal = 361,000 ± 197,000 μg/g dry weight, middle = 439,000 ± 154,000 μg/g dry weight, and distal = 616,000 ± 193,000 μg/g dry weight. As expected, collagen concentrations were higher when assayed and expressed on a dry weight basis than on a weight wet basis. In this smaller study ($n = 16$ vs. $n = 60$ in the wet weight-based study), the difference in collagen concentration between distal and proximal valves did not quite reach statistical significance.

4 Discussion

4.1 Venous valves

The prevalence of a multitude of valves (Edwards and Edwards 1940; Moore et al. 2011) throughout the venous system has been appreciated since their claimed discovery by anatomist Giambattista Canano in the 1540 s and subsequent elaboration by Fabricius ab Aquapendente and his pupil William Harvey in the early 1600 s (Franklin 1927). Thus, it is at first surprising that venous valves have received relatively little attention compared to their cardiac counterparts, despite the etiological role of venous valve incompetence in

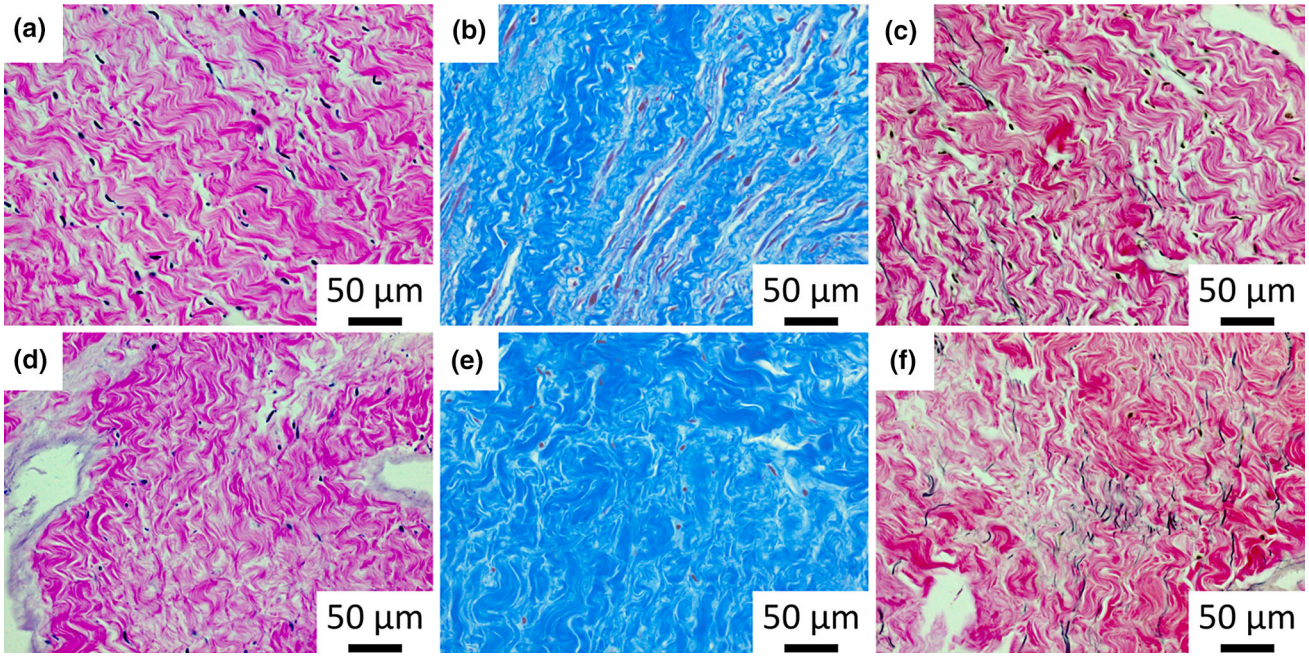

Fig. 4 Histological images of jugular venous valve tissues (400x). **a**–**c** Proximal samples stained by H&E, Masson's trichrome and VVG protocols, respectively. **d**–**f** Distal samples stained by H&E, Masson's trichrome, and VVG protocols, respectively. Collagen fiber crimp (i.e., undulations) and circumferential alignment were observed in all proximal samples, while collagen fiber alignment appeared qualitatively less pronounced in distal venous valve leaflet sections. Importantly, elastic fibers were observed in both proximal and distal VVG stained sections (panels **c** and **f**, respectively). As indicated in the Methods and in Fig. 1e, polarized light micrographs of whole-mount, unstained tissues showed that collagen fibers were oriented principally along the circumferential direction of the venous valve leaflets. In figure panels (**a**–**f**), the circumferential direction corresponds approximately with the preferred orientation of the crimped collagen fibers, with the radial direction being orthogonal to the preferred collagen fiber orientation. *Scalebars* = 50 µm

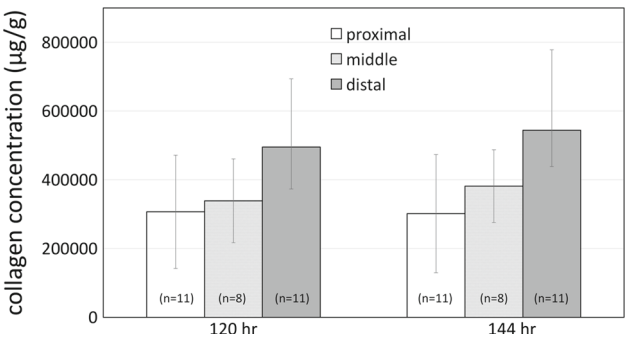

Fig. 5 Collagen concentrations measured following two different acid–pepsin extraction times (120 and 144 h). Results indicated that 120 h was sufficient to extract acetic acid–pepsin soluble collagen from bovine jugular venous valve leaflet tissues. Within both the 120- and 144-h extraction groups, a proximal-to-distal trend of increased collagen concentration was observed

CVI (Bergan 2008). The pathophysiology of venous valve incompetence in CVI is distinct from that of the semilunar heart valves and in many ways more complex. In both diseases, unidirectional blood flow is impaired, principally by regurgitant flow in venous valve failure. In the heart, incompetent valves force the heart to work harder, culminating in congestive heart failure. In the legs, venous valve incompetence lets gravity exert its full force on the column of blood between the right heart and the calves, causing distal blood pooling and stasis (risking life-threatening clots), edema, inflammation, varicose veins, damage to the lymphatic system and skin, and, in advanced CVI, venous ulcers (i.e., recurrent, non-healing wounds) (Bergan 2008).

Nevertheless, while CVI and its comorbidities claim quality of life to a degree approaching that of heart disease (Zervides and Giannoukas 2012), comparatively little attention has focused on CVI or its unique venous valvular etiology. To the best of the authors' knowledge, only a single study by Ackroyd et al. (1985) has reported on mechanical properties of venous valve leaflet tissue and only insofar as uniaxial tensile strength and failure strain. Toward addressing this critical gap in our understanding, our foremost goal in the current study was to characterize the mechanical behavior of venous valve leaflet tissues under biaxial loading.

4.2 Biaxial mechanical behavior of venous valve leaflet tissues

As evidenced by Fig. 2, the stress–strain response of venous valve leaflet tissues is highly nonlinear, characterized by toe, exponential transition, and linear regions that are typical

of soft tissues, including heart valve leaflets.[44,45] (Huang et al. 2012; Huang and Huang 2015). Such nonlinearity is not surprising, given the splayed collagen fiber orientations and undulated collagen fiber crimp observed in photomicrographs of Masson's trichrome and Verhoeff–Van Gieson stained sections (Fig. 4b, c, e, f). Indeed, the progressive recruitment of similarly rotated and undulated collagen fibers is known to shape the stress–strain response of heart valve leaflets (Hilbert et al. 1996) and bioprosthetic heart valve biomaterials (Sun et al. 2004). In our previous study on porcine aortic valves, the inflection point of the stress–strain curve occurred at a strain magnitude of ~18% strain in the circumferential direction (Huang et al. 2012). This was consistent with observations by Hilbert et al. (1996), who in uniaxial tension showed complete straightening of an ~20 μm wavelength collagen crimp at a strain of 15%. In the current study, the inflection point of the stress–strain curve occurred between 30 and 40% strain in both the circumferential and radial directions. While precise measurement of collagen fiber crimp was not undertaken in the current study, we estimated the collagen fiber crimp wavelength from our photomicrographs and obtained a value for bovine jugular vein venous valve leaflet tissue of ~40−50 μm, which would be consistent with the observed inflection point of the stress–strain curve.

Interestingly, while venous valve leaflets from the bovine jugular vein visually appeared relatively delicate compared to porcine aortic and pulmonary valve leaflets, the peak tangent moduli of venous valve leaflet tissues from bovine jugular veins were found to be significantly higher than those of porcine aortic valve leaflet tissues (e.g., 24–30 MPa for venous valves in the 45–60% strain range under equibiaxial loading versus ~1.6 MPa for the porcine aortic valve in the 28–35% strain range under equibiaxial loading Huang et al. 2012). While at first appearing counterintuitive, the higher *stiffness* of the venous valve leaflet tissue (i.e., modulus of elasticity, a normalized measure of load-bearing capacity that accounts for material thickness) can be explained in part by the venous valve leaflet's apparent lack of the glycosaminoglycan-rich spongiosa layer present in semilunar heart valve leaflets (Gottlob and May 1986). In mammalian semilunar heart valve leaflets, the central spongiosa layer has been speculated to perform a variety of functions, including elastin- and collagen-based mechanical linkage of the ventricularis layer to the collagen-dense fibrosa layer (Buchanan and Sacks 2013; Stella et al. 2007; Tseng and Grande-Allen 2011). By contrast, the relatively thin venous valve leaflets do not appear to exhibit any appreciable spongiosa-like layer (Gottlob and May 1986). Because the spongiosa layer of heart valve leaflets is comprised primarily of proteoglycans, glycosaminoglycans, and relatively low modulus elastin, the spongiosa is not expected to resist in-plane tensile loading to the same degree as the more compact fibrosa or ventricularis layers. Thus, by the venous valve leaflet comprising primarily collagens and elastin, it would be expected to be capable of supporting tensile loads to a degree more closely resembling those of the fibrosa layer of a heart valve leaflet. In support of this explanation, Liao et al. (2008) showed similarly high peak tangent moduli in decellularized porcine aortic valve leaflet tissues associated with histologically observed depletion of the spongiosa layer, with peak tangent moduli in the circumferential direction increasing from ~8 MPa (fresh) to ~20 MPa (decellularized with Triton X-100) in parallel with decreases in thickness (i.e., 0.31 ± 0.05 mm (fresh) to 0.16 ± 0.04 mm (decellularized with Triton X-100)). Offering further evidence for the role of presence or absence of the spongiosa and associated leaflet thicknesses, Engelmayr and colleagues reported a circumferential peak tangent modulus of only 1.1 MPa for bovine aortic valve leaflet tissue, at a relatively large thickness of ~1.5 mm (Masoumi et al. 2013b). Collectively, these observations suggest that on a per-weight (i.e., concentration) basis, the higher collagen concentrations measured herein for bovine jugular vein-derived venous valve leaflet tissues may contribute to their higher peak tangent moduli relative to those of heart valve leaflet tissues.[43,44] Nevertheless, other factors, including specific collagen types, cross-linking and orientation, may play a role and warrant further investigation in future studies. It is further noteworthy that peak stresses of 6.3 MPa (circumferential) and 2.5 MPa (radial) were measured at 60% strain, which were lower than the uniaxial tensile strength reported by Ackroyd et al. for human femoral vein valves (i.e., ~9 MPa Ackroyd et al. 1985). It has been shown that biaxial tensile testing data retain the influence of axial coupling, allowing for more precise predictions under generalized loading conditions. These structural and physiological loading properties confer slack and induce fiber rotations, factors, which collectively confound direct relationships between macroscale, tissue-level strain, and the state of strain within individual collagen fibers.

4.3 Collagen content of venous valve leaflet tissues

The acid–pepsin soluble collagen concentrations measured in this study for bovine jugular vein venous valve leaflet tissues (mean values ranging from 297,000 to 528,000 μg/g wet weight) were significantly higher than those we measured previously for porcine aortic or pulmonary valves (Huang et al. 2012; Huang and Huang 2015). In particular, for the belly region of aortic and pulmonary valve leaflets, we previously measured acid–pepsin soluble collagen concentrations of ~60,000 μg/g wet weight and ~80,000 μg/g wet weight, respectively (Huang et al. 2012). There are several caveats to consider in comparing results reported herein for venous valve leaflets to those of heart valve leaflets in our previous study. First, by virtue of their significantly smaller thick-

nesses, the wet weights of the venous valve leaflet samples utilized in the collagen assay (e.g., avg. 0.002 g for proximal valve samples) were lower by approximately an order of magnitude than those of the porcine aortic valve (avg. 0.0336 g) and pulmonary valve (avg. 0.0241 g) leaflet samples (Huang et al. 2012). Because the collagen concentration is normalized to the wet weight, weight measurement errors (e.g., due to water droplets) could potentially have been amplified. However, another perhaps more important consideration is that the collagen concentrations reported here for venous valve leaflet tissue and in our previous studies (Huang et al. 2012; Huang and Huang 2015) from heart valve leaflet tissues represent only the acid–pepsin- soluble fraction of the total collagen. Of note, following 120 and 144 h of acid–pepsin extraction, no remaining venous valve leaflet tissue was evident in the tube, suggesting that the majority of the collagen had been solubilized. By contrast, some residual tissue was observed in the case of aortic valve leaflet tissues in our previous studies (Huang et al. 2012; Huang and Huang 2015), suggesting the presence of insoluble collagens. Given that porcine pulmonary valves were observed to have a higher acid–pepsin soluble collagen content than corresponding aortic valves, and given the significantly lower pressures of the venous system, it is possible that pulmonary heart valve leaflets and venous valve leaflets have a larger proportion of readily soluble collagens than aortic valves. As discussed in our previous study (Huang and Huang 2015), this possibility is supported by Aldous et al. (2009), who demonstrated that the collagen of the bovine aortic valve contains a greater number of mature histidinohydroxylysinonorleucine (HHL) cross-links than that of the bovine pulmonary valve, suggesting that the aortic valve could exhibit a lower ratio of soluble to insoluble collagen. Another equally important consideration is potential species and/or vein-specific differences in venous valve leaflet collagen content. For valve-bearing, cadaveric human femoral vein, Kuna et al. (2015) recently utilized acid–pepsin solubilization and the Sircol collagen assay to measure a collagen concentration of ~1.25 μg/mg wet weight (estimated from Fig. 3c of Kuna et al. (2015), i.e., ~1250 μg/g wet weight). Of note, it was not indicated in that study whether the assay samples comprised femoral vein wall, venous valve leaflet, or a combination of the two. However, Kuna et al. (2015) utilized a tenfold lower pepsin concentration (i.e., 0.1 mg/ml pepsin vs. the 1 mg/ml utilized herein) and a significantly shorter extraction time of 48 h. In our experience with heart valve leaflets (Huang et al. 2012; Huang and Huang 2015) and leaflets from the bovine jugular vein, the lower pepsin concentration and relatively short extraction time could have resulted in the appearance of a significantly lower collagen concentration due to incomplete solubilization. In future studies, the collagen concentrations of bovine heart valves could be quantified to provide a better intra-species comparison. Nevertheless, within the context of the acid–pepsin collagen extraction protocol employed herein, a proximal-to-distal trend of increased collagen concentration was observed along the length of the bovine jugular vein valve samples (i.e., inter-valve variability). Potential physiological implications of the observed proximal-to-distal increase in jugular vein venous valve leaflet collagen concentration were not immediately apparent. We observed that the peak tangent modulus for the distal valves was on average higher than those of the proximal and middle valves, which could be consistent with the observed collagen concentrations; however, the differences in peak tangent moduli did not reach statistical significance and could have been related to other factors related to the collagen fiber microstructure.

Lastly, in the current study, only acid–pepsin soluble collagen concentrations were measured for the venous valve tissues; other potential extracellular matrix components were not quantified. For example, according to the histological images, elastin fibers were also observed in the valves (Fig. 4c, f). In the case of valve-bearing, cadaveric human femoral vein, Kuna et al. reported elastin and sulfated glycosaminoglycan concentrations of ~18 μg/mg wet weight and ~3.25 μg/mg wet weight, respectively [estimated from Fig. 3c of Kuna et al. (2015)], as well as a DNA concentration of 241.95 ± 39.44 ng/mg wet weight. However, as indicated above, it was not explicitly indicated whether these tissue samples were from the femoral vein wall, venous valve leaflet, or a combination of the two.

4.4 Implications of venous valve leaflet biaxial mechanical data on valve simulation and design

As alluded to above, the new mechanical property data made available by the current study are expected to enable more accurate simulations of native venous valve leaflets and thereby more robust prosthetic venous valve designs. The first fluid–structure interaction (FSI) model of a venous valve was presented by Buxton and Clarke (2006), in which a linear elastic, isotropic lattice spring model with a nominal spring constant of 1 MPa was employed to simulate the vein wall and leaflet tissue (of note, a local variation in spring constant magnitude was invoked on moving from the venous valve leaflet basal attachment to the free edge). Narracott et al. reported an elegant FSI computational model of a venous valve in which the mechanical properties of the venous valve leaflets were assumed to be equal to that of the vein wall (based on observations of Ackroyd et al. (1985)) and assigned linear elastic, isotropic modulus values ranging from 0.25 to 1.0 MPa at a constant leaflet thickness of 50 μm (Narracott et al. 2010). Most recently, Chen et al. (2014) reported FSI models designed to evaluate the effectiveness of mono-, bi-, and trileaflet venous valve architectures by way of a "mechanical cost function." Of note,

Chen et al. (2014) employed a nonlinear, hyperelastic strain energy density function for the venous valve leaflet tissue; however, the model modulus parameters were assumed to be equivalent to those of aortic valve leaflets. Collectively, while the above-mentioned models were each computationally rigorous and provided new insights into the mechanics of venous valve hemodynamic function, the unavailability of mechanical property data on the venous valve leaflet tissue was a significant limitation raised by the authors of each of the studies (Buxton and Clarke 2006; Chen et al. 2014; Narracott et al. 2010).

4.5 Limitations of the study

In these first efforts to quantify the biaxial mechanical properties of venous valve leaflet tissues, potential relationships between leaflet tissue mechanical properties and leaflet angular orientation (i.e., around the circumference of the jugular vein) or anatomical position relative to side branches were not explicitly evaluated. For example, while mechanical property differences were observed between individual leaflets excised from the same valve apparatus (i.e., "high" and "low" groups; Fig. 3c, d), these apparent differences did not reach statistical significances and individual leaflets comprising the "high" and "low" groups were not necessarily from the same "side" of the jugular vein (i.e., not necessarily oriented at the same angle around the jugular vein circumference). In future studies, such potential relationships will be explicitly addressed. Moreover, while peak stresses must be interpreted within the context of the applied deformation profile and the relatively limited precision [$\pm$0.001 in. (i.e., $\sim$25 μm)] of dial caliper-based thickness measurements, our goal in reporting peak stresses at 60% equibiaxial strain was to provide another measure for comparing groups (i.e., circumferential, radial, proximal, middle, and distal groups). Measures such as peak tangent modulus and peak stress do not provide a complete description; however, they enable identification of potential inter-valvular and intra-valvular variability. Another limitation of our study was that jugular vein segments obtained from the abattoir were generally of variable length. Thus, it is possible that valves classified as "middle group" could have included a combination of more centrally located proximal or distal valves, thereby contributing to the relatively higher standard deviations observed in the middle group samples.

In the current study, bovine jugular veins were used in lieu of human tissues due to their availability and use in the fabrication of prosthetic valves (Carrel 2004; McElhinney and Hennesen 2013; Zervides and Giannoukas 2012). Animal tissues can provide referential information for future clinical use in humans; however, given that differences have been observed between bovine, porcine and human *heart valve* leaflet mechanical properties (Masoumi et al. 2013a, b), there are likely differences between bovine and human venous valve leaflet tissue mechanical properties. Thus, studies on human venous valve leaflet tissues, such as that by Kuna et al. (2015), are warranted for comparison. Indeed, by virtue of anatomical and hemodynamic differences between bovines and humans, our observations regarding the distribution of bicuspid and tricuspid venous valves in bovine jugular veins do not necessarily extend across species. Likewise, it is not clear from our study or the literature how hemodynamic forces may contribute to the development and/or maintenance of one number of leaflets versus another.

As recently reviewed in detail by Bazigou and Makinen (2013), the developmental origin of venous valves was described as early as the 1920s (Kampmeier and Birch 1927). Indeed, Kampmeier and La Fleur Birch accurately indicated that bicuspid venous valve morphogenesis (in the saphenous veins) begins with transversely opposed ridges of endothelial cells that are subsequently invaded by mesenchyme (Bazigou et al. 2011). Bazigou et al. (2011) were the first to offer a complementary molecular-level description of venous valve development, showing that proteins such as ephrin-B2 and integrin-α9 are critical to venous valve formation. While not explicitly investigated, Bazigou and Makinen (2013) speculated that flow-induced forces are likely involved in venous valve formation, owing to the differential alignment of endothelial cells upstream and downstream from the venous valve. Moreover, Munger et al. (2016, 2013) showed that connexins 37, 43 and 47 are critical to venous valve formation, and Sabine (2012) showed evidence of mechanotransduction-dependent expression of connexin 37 in lymphatic valve formation. Given the parallels between venous and lymphatic valve development, it is possible that flow, and perhaps pressure, may be involved in determining the bicuspid versus tricuspid venous valve configuration. Indeed, Chen et al. (2014) recently presented biomechanical comparisons between mono-, bi-, and tricuspid venous valve configurations, showing that the common bicuspid configuration is associated with a lower mechanical "cost" (defined as the ratio of leaflet wall stress to leaflet fluid shear stress) (Chen et al. 2014).

Histological images presented in this study were obtained by way of standard brightfield (transmitted light) microscopy. For further investigation of collagen and/or cytoskeletal stress fiber orientation, tissue sections and/or whole-mount tissue samples may be imaged via fluorescence and/or confocal fluorescence microscopy. Initial histological assessments presented herein were semiquantitative and only focused on collagen fiber orientation and undulation. Further analyses, such as identifying potential pathophysiological features, were beyond the scope of the current study.

Moreover, equibiaxial tensile testing was conducted at a strain rate of 1%/s. However, such strain rates may not match the physiological loading rates (i.e., associated with

physiologic venous valve opening and closing times). As more information becomes available regarding physiological opening and closing times, the testing protocol will be adjusted accordingly.

An additional limitation was that the competence of the venous valves was not explicitly confirmed prior to leaflet excision. While venous valves were excised from the jugular veins of healthy cows following killing for meat production, it is plausible that a subset of the valves tested herein may have been regurgitant. No frank evidence of leaflet atrophy was observed in the current study; however, methods to test the competence of individual valves prior to leaflet excision will be evaluated in future studies. In particular, by adapting methods described by Franklin (1929), the jugular vein segment could be interposed between tubing on a vertical fluid column, and valve closure could be confirmed in a serial, proximal-to-distal, manner by filling the vein segment from the top of the column (i.e., from the proximal end) with a colored fluid and observing the demarcation between fluid-filled and empty vein, with the assistance of trans-illumination if needed. The jugular vein would then be dismounted from the column, resected below the line of demarcation of the competent valve, and remounted to assess the closure of downstream valves. The proximal-most segment terminating in a competent valve would then be everted and examined. If an additional valve were to be identified proximal to the competent valve, then that valve could be deemed incompetent (i.e., regurgitant).

5 Conclusions

For the first time, the nonlinear, anisotropic behavior of venous valve leaflet tissues was measured via equibiaxial mechanical loading. The peak tangent moduli of elasticity of the tissues and the peak stresses at 60% strain were obtained. The proximal leaflets exhibited significantly higher peak tangent moduli in the circumferential direction than in the radial direction, indicating that under a given pressure head, the leaflets would be expected to stretch unequally in the circumferential and radial directions during coaptation. As the venous valves were either bicuspid or tricuspid, intra-valvular variability was determined by comparing two leaflets from the same sinus location in a vein. At 60% strain, trends were observed in the peak circumferential stresses for proximal samples, with samples in the high group appearing to be appreciably higher than those in the low group. Likewise, distal samples showed trends of intra-valvular variability in the radial direction for values of both peak stress and tangent modulus of elasticity. Based on collagen assay results, a trend of increased collagen concentration was observed from proximal-to-distal valve tissues. These results indicate that valve composition could potentially be location-dependent. This new knowledge of venous valve leaflet behavior contributes important information about basic venous physiology and is critically important for the development of novel approaches to the prevention, management, rehabilitation, and repair of venous valve incompetence in CVI, such as prosthetic (de Borst and Moll 2012; de Borst et al. 2003; DeLaria et al. 1993; Hill et al. 1985; Moriyama et al. 2011; Reeves et al. 1997) and tissue-engineered venous valve replacements (Brountzos 2003; Glynn et al. 2016; Jones et al. 2012; Kehl et al. 2016; Kistner 1968; Pavcnik et al. 2000; Pavcnik 2002; Shen 2014; Teebken et al. 2003, 2009; Weber 2014; Wen 2012; Yuan 2013), surgical reconstruction techniques (Tripathi et al. 2004), design of calf muscle exercise regimens for the prevention and treatment of CVI (Padberg et al. 2004), catheter designs for minimal venous valve damage in thrombectomy (Vogel et al. 2012), and design of compression therapies to improve venous function in CVI and during pregnancy (Buchtemann et al. 1999; Chauveau et al. 2011). Thus, this study contributes toward refining our collective understanding of venous valve tissue biomechanics.

Acknowledgements The authors gratefully acknowledge Mr. George C. Engelmayr, Sr., for his assistance in sourcing bovine jugular vein tissues and Adam Benson for performing collagen assays on lyophilized valve tissues. This work was supported by NSF CBET-1553430.

Compliance with ethical standards

Conflict of interest The authors declare that they have no conflict of interest.

References

Ackroyd JS, Pattison M, Browse NL (1985) A study of the mechanical properties of fresh and preserved human femoral vein wall and valve cusps. Br J Surg 72:117–119

Aldous IG, Veres SP, Jahangir A, Lee JM (2009) Differences in collagen cross-linking between the four valves of the bovine heart: a possible role in adaptation to mechanical fatigue. Am J Physiol Heart Circ Physiol 296:H1898–1906. doi:10.1152/ajpheart.01173.2008

Bazigou E, Lyons OT, Smith A, Venn GE, Cope C, Brown NA, Makinen T (2011) Genes regulating lymphangiogenesis control venous valve formation and maintenance in mice. J Clin Investig 121:2984–2992. doi:10.1172/JCI58050

Bazigou E, Makinen T (2013) Flow control in our vessels: vascular valves make sure there is no way back. Cell Mol Life Sci 70:1055–1066. doi:10.1007/s00018-012-1110-6

Beebe-Dimmer JL, Pfeifer JR, Engle JS, Schottenfeld D (2005) The epidemiology of chronic venous insufficiency and varicose veins. Ann Epidemiol 15:175–184. doi:10.1016/j.annepidem.2004.05.015

Bergan JJ (2008) Venous valve incompetence: the first culprit in the pathophysiology of chronic venous insufficiency. Medicographia 30:87–94

Bernardini E, De Rango P, Piccioli R, Bisacci C, Pagliuca V, Genovese G, Bisacci R (2010) Development of primary superficial venous insufficiency: the ascending theory. Observational and hemody-

namic data from a 9-year experience. Ann Vasc Surg 24:709–720. doi:10.1016/j.avsg.2010.01.011

Billiar KL, Sacks MS (2000) Biaxial mechanical properties of the natural and glutaraldehyde treated aortic valve cusp—part I: experimental results. J Biomech Eng 122:23–30

Brountzos E et al (2003) Remodeling of suspended small intestinal submucosa venous valve: an experimental study in sheep to assess the host cells' origin. J Vasc Interv Radiol 14:349–356. doi:10.1097/01.Rvi.0000058410.01661.62

Buchanan RM, Sacks MS (2013) Interlayer micromechanics of the aortic heart valve leaflet. Biomech Model Mechanobiol. doi:10.1007/s10237-013-0536-6

Buchtemann AS, Steins A, Volkert B, Hahn M, Klyscz T, Junger M (1999) The effect of compression therapy on venous haemodynamics in pregnant women. Br J Obstetri Gynaecol 106:563–569

Buescher CD, Nachiappan B, Brumbaugh JM, Hoo KA, Janssen HF (2005) Experimental studies of the effects of abnormal venous valves on fluid flow. Biotechnol Prog 21:938–945. doi:10.1021/bp049835u

Buxton GA, Clarke N (2006) Computational phlebology: the simulation of a vein valve. J Biol Phys 32:507–521. doi:10.1007/s10867-007-9033-4

Carrel T (2004) Bovine valved jugular vein (Contegra^{TM}) to reconstruct the right ventricular outflow tract. Expert Rev Med Devices 1:11–19. doi:10.1586/17434440.1.1.11

Chauveau M, Gelade P, Cros F (2011) The venous return simulator: comparison of simulated with measured ambulatory venous pressure in normal subjects and in venous valve incompetence. VASA Z Gefasskrankh 40:205–217. doi:10.1024/0301-1526/a000095

Chen HY, Berwick Z, Krieger J, Chambers S, Lurie F, Kassab GS (2014) Biomechanical comparison between mono-, bi-, and tricuspid valve architectures. J Vasc Surg Venous Lymphat Disord 2:188–193. doi:10.1016/j.jvsv.2013.08.004

Corno AF, Hurni M, Griffin H, Jeanrenaud X, von Segesser LK (2001) Glutaraldehyde-fixed bovine jugular vein as a substitute for the pulmonary valve in the Ross operation. J Thorac Cardiovasc Surg 122:493–494. doi:10.1067/mtc.2001.114780

Davis FM, De Vita R (2012) A nonlinear constitutive model for stress relaxation in ligaments and tendons. Ann Biomed Eng 40:2541–2550. doi:10.1007/s10439-012-0596-2

de Borst GJ, Moll FL (2012) Percutaneous venous valve designs for treatment of deep venous insufficiency. J Endovasc Ther 19:291–302. doi:10.1583/11-3766R.1

de Borst GJ, Teijink JA, Patterson M, Quijano TC, Moll FL (2003) A percutaneous approach to deep venous valve insufficiency with a new self-expanding venous frame valve. J Endovasc Ther 10:341–349. doi:10.1177/152660280301000227

DeLaria GA, Phifer T, Roy J, Tu R, Thyagarajan K, Quijano RC (1993) Hemodynamic evaluation of a bioprosthetic venous prosthesis. J Vasc Surg 18:577–584 (**discussion 584-576**)

Edwards JE, Edwards EA (1940) The saphenous valves in varicose veins. Am Heart J 19:338

Engelmayr GC Jr, Rabkin E, Sutherland FW, Schoen FJ, MJ E Jr, Sacks MS (2005) The independent role of cyclic flexure in the early in vitro development of an engineered heart valve tissue. Biomaterials 26:175–187

Fan CM (2005) Venous pathophysiology. Semin Intervent Radiol 22:157–161. doi:10.1055/s-2005-921949

Franklin K (1927) Valves in veins: an historical survey. Proc R Soc Med 21:1–33

Franklin K (1929) Valves in veins: further observations. J Anat 64:67–69

Glynn JJ, Jones CM, Anderson DEJ, Pavcnik D, Hinds MT (2016) In vivo assessment of two endothelialization approaches on bioprosthetic valves for the treatment of chronic deep venous insufficiency. J Biomed Mater Res B 104:1610–1621. doi:10.1002/jbm.b.33507

Gottlob R, May R (1986) Venous valves: morphology, function, radiology, surgery. Springer-Verlag, Wien, New York

Hilbert SL, Sword LC, Batchelder KF, Barrick MK, Ferrans VJ (1996) Simultaneous assessment of bioprosthetic heart valve biomechanical properties and collagen crimp length. J Biomed Mater Res 31:503–509. doi:10.1002/(Sici)1097-4636(199608)31:4<503::Aid-Jbm10>3.0.Co;2-H

Hill R, Schmidt S, Evancho M, Hunter T, Hillegass D, Sharp W (1985) Development of a prosthetic venous valve. J Biomed Mater Res 19:827–832. doi:10.1002/jbm.820190708

Huang H-YS, Balhouse BN, Huang S (2012) Application of simple biomechanical and biochemical tests to heart valve leaflets: implications for heart valve characterization and tissue engineering. Proc Inst Mech Eng Part H 226:868–876. doi:10.1177/0954411912455004

Huang H-YS, Huang S, Frazier CP, Prim P, Harrysson O (2014) Directional mechanical property of porcine skin tissues. J Mech Med Biol. doi:10.1142/S0219519414500699

Huang H-YS, Liao J, Sacks MS (2007) In-situ deformation of the aortic valve interstitial cell nucleus under diastolic loading. J Biomech Eng Trans ASME 129:880–889. doi:10.1115/1.2801670

Huang S, Huang H-YS (2015) Biaxial stress relaxation of semilunar heart valve leaflets during simulated collagen catabolism: effects of collagenase concentration and equibiaxial strain-state. Proc Inst Mech Eng Part H 229:721–731. doi:10.1177/0954411915604336

James KV, Lohr JM, Deshmukh RM, Cranley JJ (1996) Venous thrombotic complications of pregnancy. Cardiovasc Surg 4:777–782

Jones CM, Hinds MT, Pavcnik D (2012) Retention of an autologous endothelial layer on a bioprosthetic valve for the treatment of chronic deep venous insufficiency. J Vasc Interv Radiol 23:697–703. doi:10.1016/j.jvir.2012.01.062

Kampmeier OF, Birch CLF (1927) The origin and development of the venous valves, with particular reference to the saphenous district. Am J Anat 38:451–499. doi:10.1002/aja.1000380306

Karino T, Motomiya M (1984) Flow through a venous valve and its implication for thrombus formation. Thrombosis Res 36:245–257

Kehl D, Weber B, Hoerstrup SP (2016) Bioengineered living cardiac and venous valve replacements: current status and future prospects. Cardiovasc Pathol 25:300–305. doi:10.1016/j.carpath.2016.03.001

Kistner RL (1968) Surgical repair of a venous valve. Straub Clin Proc 34:41–43

Kuna VK et al (2015) Successful tissue engineering of competent allogeneic venous valves. J Vasc Surg Venous Lymphat Disord 3:421–430. doi:10.1016/j.jvsv.2014.12.002

Liao J, Joyce EM, Sacks MS (2008) Effects of decellularization on the mechanical and structural properties of the porcine aortic valve leaflet. Biomaterials 29:1065–1074. doi:10.1016/j.biomaterials.2007.11.007

Lochner P, Nedelmann M, Kaps M, Stolz E (2014) Jugular valve incompetence in transient global amnesia. A problem revisited. J Neuroimaging 24:479–483. doi:10.1111/jon.12042

Lurie F, Kistner RL, Eklof B, Kessler D (2003) Mechanism of venous valve closure and role of the valve in circulation: a new concept. J Vasc Surg 38:955–961. doi:10.1016/S0741

Masoumi N, Jean A, Zugates JT, Johnson KL, Engelmayr GC (2013) Laser microfabricated poly (glycerol sebacate) scaffolds for heart valve tissue engineering. J Biomed Mater Res Part A 101:104–114. doi:10.1002/Jbm.A.34305

Masoumi N, Johnson KL, Howell MC, Engelmayr GC Jr (2013) Valvular interstitial cell seeded poly (glycerol sebacate) scaffolds: toward a biomimetic in vitro model for heart valve tissue engineering. Acta Biomater 9:5974–5988. doi:10.1016/j.actbio.2013.01.001

May-Newman K, Lam C, Yin FCP (2009) A hyperelastic constitutive law for aortic valve tissue. J Biomech Eng. doi:10.1115/1.3127261

McElhinney DB, Hennesen JT (2013) The Melody® valve and Ensemble® delivery system for transcatheter pulmonary valve replacement. Ann NY Acad Sci 1291:77–85. doi:10.1111/nyas.12194

Moore HM, Gohel M, Davies AH (2011) Number and location of venous valves within the popliteal and femoral veins: a review of the literature. J Anat 219:439–443. doi:10.1111/j.1469-7580.2011.01409.x

Moriyama M, Kubota S, Tashiro H, Tonami H (2011) Evaluation of prosthetic venous valves, fabricated by electrospinning, for percutaneous treatment of chronic venous insufficiency. J Artif Organs 14:294–300. doi:10.1007/s10047-011-0588-2

Munger SJ, Geng X, Srinivasan RS, Witte MH, Paul DL, Simon AM (2016) Segregated Foxc2, NFATc1 and Connexin expression at normal developing venous valves, and Connexin-specific differences in the valve phenotypes of Cx37, Cx43, and Cx47 knockout mice. Dev Biol 412:173–190. doi:10.1016/j.ydbio.2016.02.033

Munger SJ, Kanady JD, Simon AM (2013) Absence of venous valves in mice lacking Connexin37. Dev Biol 373:338–348. doi:10.1016/j.ydbio.2012.10.032

Narracott AJ, Zervides C, Diaz V, Rafiroiu D, Lawford PV, Hose DR (2010) Analysis of a mechanical heart valve prosthesis and a native venous valve: two distinct applications of FSI to biomedical applications. Int J Numer Methods Biomed Eng 26:421–434

Nedelmann M, Kaps M, Mueller-Forell W (2009) Venous obstruction and jugular valve insufficiency in idiopathic intracranial hypertension. J Neurol 256:964–969. doi:10.1007/s00415-009-5056-z

Noishiki Y et al (1993) Development and evaluation of a pliable biological valved conduit. 1. Preparation, biochemical-properties, and histological-findings. Int J Artif Organs 16:192–198

Padberg FT Jr, Johnston MV, Sisto SA (2004) Structured exercise improves calf muscle pump function in chronic venous insufficiency: a randomized trial. J Vasc Surg 39:79–87. doi:10.1016/j.jvs.2003.09.036

Pavcnik D, Uchida BT, Timmermans H, Corless CL, Keller FS, Rosch J (2000) Aortic and venous valve for percutaneous insertion. Minim Invasive Ther Allied Technol 9:287–292. doi:10.1080/13645700009169659

Pavcnik D et al (2002) Percutaneous bioprosthetic venous valve: a long-term study in sheep. J Vasc Surg 35:598–602. doi:10.1067/mva.2002.118825

Qui Y, Quijano RC, Wang SK, Hwang NH (1995) Fluid dynamics of venous valve closure. Ann Biomed Eng 23:750–759

Qureshi MI et al (2015) A study to evaluate patterns of superficial venous reflux in patients with primary chronic venous disease. Phlebology 30:455–461. doi:10.1177/0268355514536384

Reeves TR, Cezeaux JL, Sackman JE, Cassada DC, Freeman MB, Stevens SL, Goldman MH (1997) Mechanical characteristics of lyophilized human saphenous vein valves. J Vasc Surg 26:823–828

Rittgers SE, Oberdier MT, Pottala S (2007) Physiologically-based testing system for the mechanical characterization of prosthetic vein valves. Biomed Eng Online 6:29. doi:10.1186/1475-925X-6-29

Sabine A et al (2012) Mechanotransduction, PROX1, and FOXC2 cooperate to control connexin37 and calcineurin during lymphatic-valve formation. Dev Cell 22:430–445. doi:10.1016/j.devcel.2011.12.020

Shen MR et al (2014) Biocompatibility evaluation of tissue-engineered valved venous conduit by reseeding autologous bone marrow-derived endothelial progenitor cells and multipotent adult progenitor cells into heterogeneous decellularized venous matrix. J Tissue Eng Regen Med. doi:10.1002/term.1877

Sparey C, Haddad N, Sissons G, Rosser S, de Cossart L (1999) The effect of pregnancy on the lower-limb venous system of women with varicose veins. Eur J Vasc Endovasc Surg 18:294–299. doi:10.1053/ejvs.1999.0870

Stella JA, Liao J, Sacks MS (2007) Time-dependent biaxial mechanical behavior of the aortic heart valve leaflet. J Biomech 40:3169–3177. doi:10.1016/j.jbiomech.2007.04.001

Sun W, Sacks M, Fulchiero G, Lovekamp J, Vyavahare N, Scott M (2004) Response of heterograft heart valve biomaterials to moderate cyclic loading. J Biomed Mater Res A 69:658–669. doi:10.1002/jbm.a.30031

Teebken OE, Puschmann C, Aper T, Haverich A, Mertsching H (2003) Tissue-engineered bioprosthetic venous valve: a long-term study in sheep. Eur J Vasc Endovasc Surg 25:305–312. doi:10.1053/ejvs.2002.1873

Teebken OE, Puschmann C, Breitenbach I, Rohde B, Burgwitz K, Haverich A (2009) Preclinical development of tissue-engineered vein valves and venous substitutes using re-endothelialised human vein matrix. Eur J Vasc Endovasc Surg 37:92–102. doi:10.1016/j.ejvs.2008.10.012

Tripathi R, Sieunarine K, Abbas M, Durrani N (2004) Deep venous valve reconstruction for non-healing leg ulcers: techniques and results. ANZ J Surg 74:34–39

Tseng H, Grande-Allen KJ (2011) Elastic fibers in the aortic valve spongiosa: a fresh perspective on its structure and role in overall tissue function. Acta Biomater 7:2101–2108. doi:10.1016/j.actbio.2011.01.022

van Geemen D, Driessen-Mol A, Grootzwagers LGM, Soekhradj-Soechit RS, Vis PWR, Baaijens FPT, Bouten CVC (2012) Variation in tissue outcome of ovine and human engineered heart valve constructs: relevance for tissue engineering. Regen Med 7:59–70. doi:10.2217/rme.11.100

Vogel D, Walsh ME, Chen JT, Comerota AJ (2012) Comparison of vein valve function following pharmacomechanical thrombolysis versus simple catheter-directed thrombolysis for iliofemoral deep vein thrombosis. J Vasc Surg 56:1351–1354. doi:10.1016/j.jvs.2012.02.053

Weber B et al (2014) Living-engineered valves for transcatheter venous valve repair. Tissue Eng Part C Methods. doi:10.1089/ten.TEC.2013.0187

Wen Y et al (2012) Construction of tissue-engineered venous valves in vitro using two types of progenitor cells and decellularized scaffolds category: original article. Open Tissue Eng Regen Med J 5:9–16. doi:10.2174/1875043501205010009

Yuan JM et al (2013) Functional analysis in vivo of engineered valved venous conduit with decellularized matrix and two bone marrow-derived progenitors in sheep. J Tissue Eng Regen Med. doi:10.1002/term.1748

Zervides C, Giannoukas AD (2012) Historical overview of venous valve prostheses for the treatment of deep venous valve insufficiency. J Endovasc Ther 19:281–290. doi:10.1583/11-3594MR.1